



OPEN Preparation and characterization of calcium-doped graphene oxide-chitosan Nanocarrier to enhance the gene delivery in MCF-7 cell line

Amirreza Diari Bidgoli¹, Abbas Farmany², Mohammad Taheri³, Meysam Soleimani¹ & Fatemeh Nouri¹✉

Gene delivery has emerged as a novel and effective method in the treatment of malignancies within medical interventions by applying nanotechnology. Consequently, the development of appropriate nanocarriers is a key focus of this research. Dynamic light scattering (DLS), fourier transform infrared (FT-IR) spectroscopy, x-ray diffraction (XRD), and thermal gravimetric analysis (TGA) were employed for the characterization of the synthesized nanocarrier. Furthermore, to assess the gene transfer capability of the nanocarrier, various techniques such as gel retardation assay, nuclease resistance assay, cytotoxicity assay, flow cytometry, and transfection were employed. The average particle size and zeta potential of the GO-CS@Ca nanocarrier were obtained as 319.8 nm and +92.8 mv, respectively. In the gel retardation test, it was observed that pDNA was effectively condensed by the GO-CS@Ca nanocarrier. The results of the MTT assay indicated that both GO-CS@Ca nanocarrier and the GO-CS@Ca/pDNA nanoplex with low toxicity. In flow cytometry analysis, it was observed that the complexation of pDNA with the GO-CS@Ca nanocarrier resulted in effective gene delivery to the MCF-7 cell line and consequently increased apoptosis induction.

Keywords Graphene-oxide, Chitosan, Breast cancer, MCF-7 cell line, Gene delivery, Nanocarrier

Abbreviations

GO	Graphene oxide
CS	Chitosan
GO-CS@Ca	Graphene oxide-chitosan-calcium

Breast cancer is a major health issue, and ranks as the second leading cause of cancer-related deaths in women, following lung cancer. In 2022, over 4 million cases of breast cancer were reported in the United States^{1,2}. Chemotherapy utilizes mechanisms such as binding to microtubules and their inhibition, microtubule depolymerization, disruption of the mitosis process, inhibition of topoisomerase, and inducing DNA damage through alkylating agents, incorporation of antimetabolites into DNA structure, and prevention of DNA replication³. On the other hand, radiotherapy is used as a valuable therapeutic approach by directly damaging the DNA structure using ionizing radiation⁴. Influx/efflux systems, by reducing the drug load inside the cells and pumping the entered drugs out of the cell membrane with the help of p-glycoprotein activity on the one hand, and DNA damage repair processes on the other hand, lead to drug resistance and a decrease in the effectiveness of chemotherapy⁵. In addition, in radiotherapy, the presence of genes such as XRCC1, RPA, and PARPs, along with processes like cell redistribution involving cellular repair, and the presence of processes such as epithelial to mesenchymal transition (EMT), contribute to increased recurrence and ultimately the development of treatment resistance⁴. Furthermore, the common side effects of therapies and unintended damage to non-cancerous tissues due to inappropriate targeting necessitate the urgent development of novel therapeutic approaches. Due to innovative methods in nanotechnology and the use of nanocarriers, the effectiveness of treatment has significantly increased^{2,6}. The use of nanoparticles as implants with immunomodulatory properties or for directly inducing apoptosis in cancerous cell membranes is under investigation. Additionally, nanoparticles

¹Department of Pharmaceutical Biotechnology, School of Pharmacy, Hamadan University of Medical Sciences, Hamadan, Iran. ²Dental Implant Research Center, Dental School, Hamadan University of Medical Sciences, Hamadan, Iran. ³Department of Medical Microbiology, School of Medicine, Hamadan University of Medical Sciences, Hamadan, Iran. ✉email: Fatemenouri1@gmail.com

are recognized as suitable carriers for drug delivery and gene delivery due to their high bioavailability and high surface-to-volume ratio⁷. The use of gene delivery systems expressing apoptotic proteins is considered an effective approach to treating malignant phenotypes. By achieving maximal gene transfer into the target cell population, inducing multiple apoptotic pathways, and combining it with chemotherapy and radiotherapy, it leads to an increased cellular death outcome⁸. Gene therapy works by intervening in gene function, either by restoring gene activity or silencing a specific gene⁹. In this study, the pro-apoptotic gene BID (a human pro-apoptotic gene that induces apoptosis very rapidly and efficiently, as a suicide gene) was used for gene delivery. The protein tBID (a selective inhibitor of homeodomain-interacting protein kinase 2 (HIPK2)) acts as a suppressor of the BCL-2 gene. The BCL-2 family of proteins is among the most important regulators of the apoptosis process, and their overexpression in cancer cells delays the apoptosis process¹⁰. In the conducted study, a non-viral polymeric carrier based on graphene oxide-chitosan was utilized for gene delivery. Graphene oxide is a two-dimensional carbon-based structure obtained from graphite powder through the Hummers method, and it exhibits various physicochemical properties such as biocompatibility, rapid performance, and a large surface area for drug loading, making it widely applicable in drug delivery and gene delivery^{11–13}. Chitosan, is a biocompatible and biodegradable polymer that, when conjugated with graphene oxide, provides a suitable platform for gene transfer due to its negative charge¹⁴. Furthermore, calcium was utilized for filling the cavities of the graphene oxide-chitosan nanocomposite and exposing the transferred gene on its surface. This study investigates the synthesis, characterization, and evaluation of a graphene oxide-chitosan-calcium doped nanocomposite for gene delivery to the MCF-7 cell line.

Materials and methods

Materials

MTT, N-hydroxybenzotriazole, 1-ethyl-3-[3-dimethylaminopropyl] carbodiimide hydrochloride, 1-hydroxybenzotriazole hydrate, and N-[2-hydroxyethyl] piperazine-N-[2-ethanesulfonic acid] (HEPES) and Chitosan were purchased from Sigma-Aldrich (Munich, Germany). Cell culture experiments were performed using FBS and DMEM (Gibco, Gaithersburg, MD, USA). Spectra/Por dialysis membrane was obtained from Spectrum Laboratories (Houston, TX, USA). All solvents and chemicals were purchased from Sigma-Aldrich (Munich, Germany) and were of the highest purity available.

Synthesis of GO

Graphene oxide is prepared according to the modified Hummers method with a little modification. Briefly, 1 g of graphite powder was mixed with 100 mL of 98% sulfuric acid. The mixture was placed on a magnetic stirrer with a speed of 26 rpm for 5 h at a temperature of 80 °C. Then, 6 g of potassium permanganate was slowly added to the mixture in an ice bath, and the stirring was continued for 2 h. Then, 100 mL of deionized water at a controlled temperature (below 60 °C) is added to the mixture under a laminar hood (to prevent the risk of gas evolution). Afterward, it is diluted again with 100 mL of deionized water and mixed with 6 mL of hydrogen peroxide to neutralize the remaining potassium permanganate, and the mixture is stirred overnight. Next, the mixture is sonicated for 30 min using an ultrasonic probe and transferred to Falcon tubes. The tubes are then centrifuged at 4000 rpm for 20 min. This step is repeated several times. The obtained supernatant is centrifuged at 8500 rpm for 15 min to collect the graphene oxide sediment¹⁵.

GO-Chitosan nanocomposite synthesis

To activate chitosan, a process involving the following steps was employed: 40 g of chitosan was added to 96 ml of 3% acetic acid. The mixture was stirred continuously for 4–5 h until the chitosan completely dissolved. As a result, a homogeneous gel-like mass was obtained, indicating successful pre-activation of the chitosan. 100 mg GO was added to 500 mg of chitosan in a (2-(N-morpholino)ethanesulfonic acid (MES) buffer with a concentration of 1.95 w/v%. After 10 min of stirring, the mixture was transferred to an ultrasonic bath for 15 min. Then, to activate chitosan to conjugate with GO, 250 mg of N-Hydroxysuccinimide (NHS) and 200 mL of 1-ethyl-3-[3-(dimethylamino)propyl]carbodiimide (EDC) were added to it, and after 10 min of stirring, it was sonicated again for 15 min to obtain the GO-CS nanocomposite. The final mixture was placed on a stirrer overnight.

Calcium doping of the graphene oxide-chitosan nanocomposite

To the GO-CS mixture, 0.1 M acetic acid was added, followed by the addition of 100 mg of calcium chloride dissolved in 2 mL of distilled water. Throughout the entire process, the mixture was stirred slowly with a magnetic stirrer. Then, the container was covered with paraffin wax, and the stirring speed was increased. In the final step, the activated dialysis bag was washed with deionized water, and the mixture was poured into it. Subsequently, it was stirred overnight. Then, the mixture was freeze-dried to obtain the calcium-doped graphene oxide-chitosan nanocomposite.

Characterization of nanocarrier

The average particle size and surface charge of the nanocarrier were measured. After dispersing the nanocarrier in water at a temperature of 25 °C, the measurements were conducted using the Horiba SZ-100 instrument (Japan). The nanocarrier structure was confirmed utilizing Fourier transform infrared (FT-IR) spectroscopy in the 450–4000 cm⁻¹ range with the PerkinElmer X FTIR Spectrometer-1720 instrument. The crystal structure of the sample was examined using X-ray diffraction (XRD) analysis with the Bruker D8 Advance instrument, and the resulting diffraction pattern was recorded. The changes in the characteristics of the studied nanocomposite due to heat were investigated using thermal gravimetric analysis (TGA) with the TGA Q600 instrument. The measurements were conducted in the temperature range of 40 to 80 °C, with a heating rate of 10 °C/min in an air atmosphere, and the corresponding TGA curve was recorded.

Gel retardation (DNA condensation) assay

To condense the pDNA (Naked pDNA) using a nanocarrier and evaluate the quality of nanocarrier-gene interaction, electrophoresis gel testing was utilized. GO-CS@Ca/pDNA (BID) nanoplex were poured into wells of a 1% agarose gel at different concentrations. Electrophoresis was performed at a voltage of 90 mv for 30 min, and the results were examined using a gel documentation device (Gel-Duc).

Protection against DNase I assay

Electrophoresis using a 1% agarose gel was employed to investigate the degree of DNA protection (similar gel retardation assay) offered by the nanocarrier against the DNase I enzyme. To prepare the samples, initially, 4 μ L of plasmid DNA (BID), 6 μ L of injectable water, and the predetermined concentrations of the nanocarrier were added to each microtube. Subsequently, the mixture was combined with 10 μ L of DNase I enzyme (1U/L) and incubated for 30 min at 37°C temperature. Finally, to neutralize the enzyme, 4 μ L of EDTA (50 mM) was added, and the mixture was incubated at a temperature of 65°C for 10 min.

Cell culture

MCF-7 cell line was purchased from Iran Pasteur Institute and cultured in T25 flasks using Dulbecco's Modified Eagle Medium (DMEM) supplemented with 10% fetal bovine serum (FBS) and 1% penicillin-streptomycin mixture. The cells were cultured in an incubator containing 5% carbon dioxide at a temperature of 37°C.

Cytotoxicity assay using MTT assay

To evaluate the cellular toxicity of the nanocarrier alone and in complex with pDNA, the MTT assay was conducted at 24 and 48 h. The cultured cells were kept in the incubator at 37°C for 24 h. Afterward, the culture medium was replaced with a fresh medium. After 72 h, if the cell confluency exceeded 80%, the cells were removed from the flask and counted using a Neubauer chamber under a microscope. Subsequently, 7000 cells were added to each well of a 96-well microplate, and the cells were incubated for 24 h. Then, both the GO-CS@Ca nanocarrier and GO-CS@Ca/pDNA (BID) nanoplex, with an initial concentration of 1 mg/mL, were serially diluted at a 1:2 ratio. Four replicates were considered for each concentration. After adding the prepared samples to the wells, 20 μ L of MTT solution was added to each well at two time points, 24 and 48 h after removing the microplate from the culture medium. After 4 h of incubation, the MTT solution was aspirated, and 100 μ L of DMSO was added to each well. The absorption was measured at 570 nm using an ELISA reader. Finally, the measured optical densities (OD) are converted to cell viability percentages using the following formula:

$$\text{Cell viability (\%)} = \frac{\text{Mean OD}_{\text{sample}}}{\text{Mean OD}_{\text{blank}}} \times 100$$

Apoptosis evaluation by flow cytometry

To evaluate the apoptosis process, 250,000 cells were seeded in each well of a 6-well plate on the morning of the first day. On the following day, after performing the treatments with 1 mg/mL of the control, control/pDNA (BID) nanoplex, GO-CS@Ca nanocarrier, and GO-CS@Ca/pDNA (BID) nanoplex, the cells were trypsinized and centrifuged for 5 min. To the cell pellet obtained from centrifugation, 10 μ L of propidium iodide (PI) dye and 5 μ L of Annexin-V dye were added, and then all contents were mixed by gently shaking the microtube. In the next step, the samples were incubated in darkness at room temperature (25°C) for 10 min. Finally, cellular analysis was performed using a flow cytometer.

Cell cycle evaluation by flow cytometry

First, a total of 250,000 cells were seeded in each well of 6-well plates, and the treatments were performed using 1 mg/mL of control, control/pDNA (BID) nanoplex, GO-CS@Ca nanocarrier, and GO-CS@Ca/pDNA (BID) nanoplex. Subsequently, to assess cell cycle ratios and the DNA content of fragmented pieces resulting from apoptosis, the cell trypsinization, and centrifugation steps were carried out for 5 min. Then, the cells were resuspended in 1 mL of 70% ethanol and fixed with 100 μ L of buffer at 4°C. To be read by the flow cytometer, the samples were centrifuged twice for 5 min, and then a mixture of 10 μ L of PI dye, 0.5 μ L of RNase, and 189.5 μ L of PBS buffer was added to the pellet obtained from centrifugation and incubated at 37°C for 25 min.

Cell transfection

A total of 250,000 cells were seeded in each well of 6-well plates, and after reaching 80% confluency, they were treated with GO-CS@Ca/pDNA (GFP) nanoplex similar to flow cytometry assay. Finally, the penetration of the desired nanoplex into the cell was assessed using the green wavelength range of the fluorescent microscope.

Statistical analysis

Statistical analyses were conducted using GraphPad Prism and SPSS software, employing the One-way ANOVA test. Results with $P \leq 0.05$ were considered statistically significant.

Results

Synthesis and characterization of nanocarrier

In the DLS analysis, the average particle size of the GO-CS@Ca nanocarrier was measured to be 319.8 nm, and the PDI (Polydispersity Index) was calculated to assess the uniformity of the nanocarrier dispersion, resulting in a value of 0.199, which falls within an acceptable range for polymer-based nanoparticles (<0.2)¹⁶. The zeta potential of the nanocarrier was measured to be +92.8 mV, attributed to the presence of amino groups on the chitosan surface.

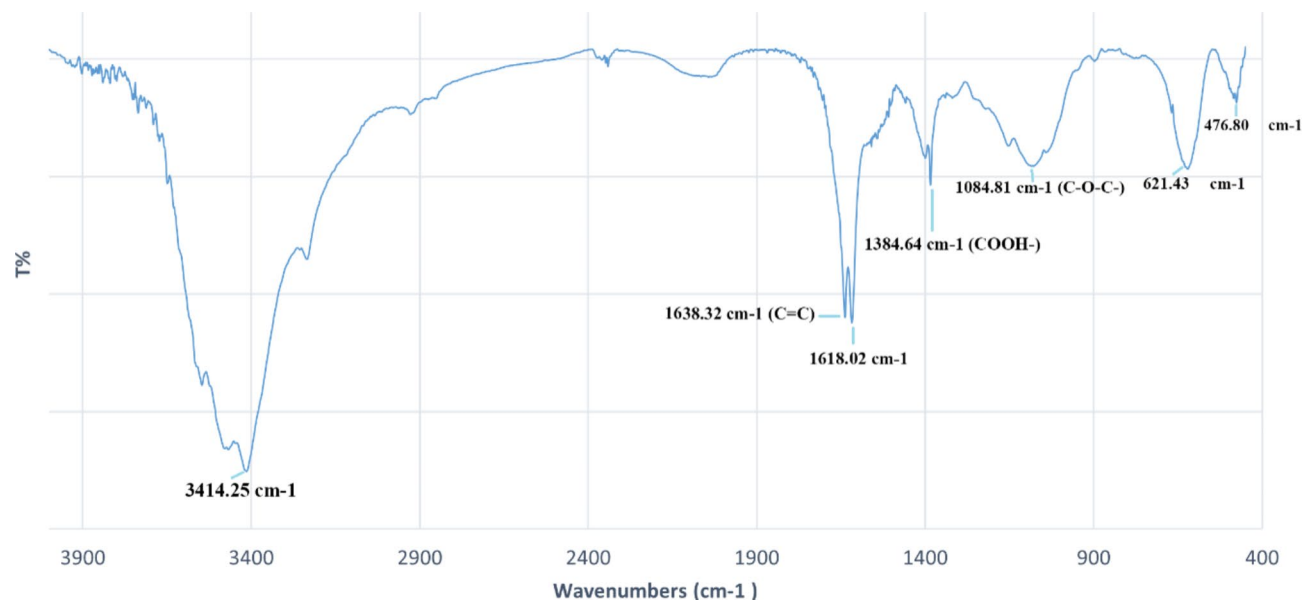


Fig. 1. FT-IR spectra of GO-CS@Ca.

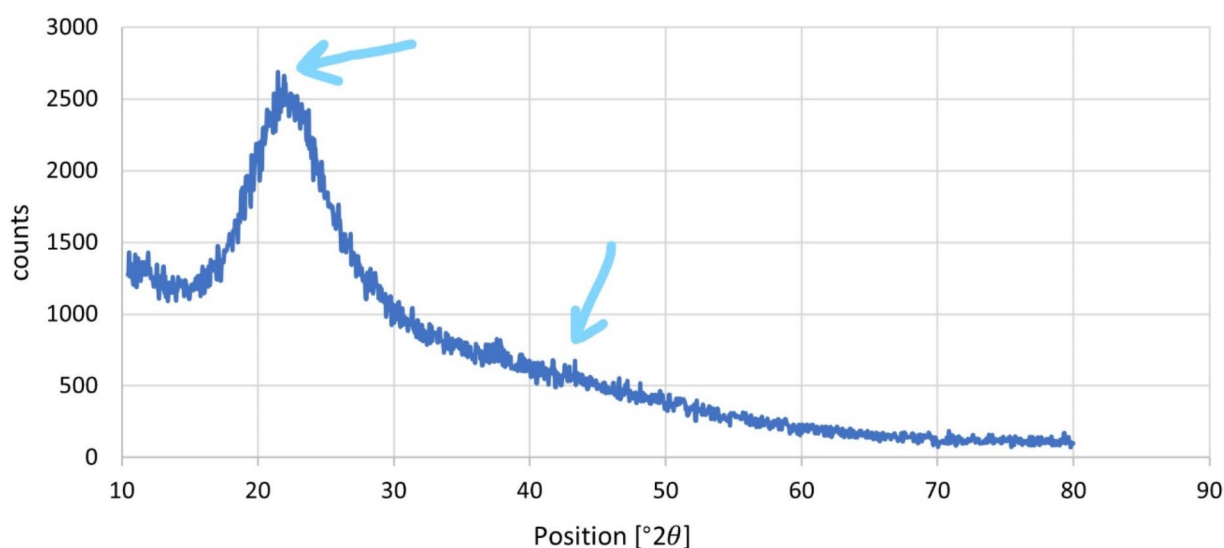


Fig. 2. XRD pattern of GO-CS@Ca.

FT-IR analysis

The FTIR analysis of the graphene oxide-chitosan composite revealed a noticeable decrease in intensity for the peak at 3414 cm^{-1} and the band between 2800 cm^{-1} and 3100 cm^{-1} when compared to the original multilayer graphene oxide. The presence of sp^2 -hybridization of $\text{C}=\text{C}$ in the graphene structure was confirmed by the peak observed at 1638 cm^{-1} . Epoxy groups ($-\text{C}-\text{O}-\text{C}-$) were identified by the band between 1106 cm^{-1} and 1084 cm^{-1} . Carboxylic groups ($-\text{COOH}-$) were detected by the peak at 1384 cm^{-1} . Additionally, a peak at 2300 cm^{-1} corresponded to the presence of absorbed CO_2 molecules (Fig. 1).

XRD analysis

X-ray diffraction (XRD) pattern of graphene displayed a characteristic diffraction peak known as the “G” peak at around $2\theta=23^\circ$ which corresponds to the in-plane sp^2 carbon-carbon bonding in the graphene lattice (Fig. 2). Another prominent peak observed in the XRD pattern of graphene is the “2D” peak. This peak appears at around $2\theta=44^\circ$ and represents the second-order Raman scattering of the graphene lattice. The XRD pattern of synthesized graphene is generally characterized by sharp, well-defined peaks, indicating its high crystallinity and well-ordered atomic arrangement.

TGA analysis

Thermogravimetric analysis (TGA) of graphene-chitosan composite provides valuable information about its thermal stability and decomposition behavior. The TGA curve obtained from the analysis reveals distinct features indicating the weight loss and thermal degradation of the composite material. The TGA curve might show an initial weight loss at below 100 °C, which can be attributed to the evaporation of moisture or volatile components present in the composite and/or evaporation of the adsorbed water in the π -stacking of GO. Following the initial weight loss, a stable region was observed where the weight remained relatively constant. This indicates the presence of thermally stable components in the composite. During the TGA analysis of the graphene-chitosan composite, a distinct second abrupt mass loss stage is observed within the temperature range of approximately 150 °C to 250 °C. This mass loss can be primarily attributed to the pyrolysis and decomposition of oxygen-containing functional groups present in graphene oxide (GO) (Fig. 3).

The ability of the GO-CS@Ca nanocarrier to condense and protect the gene structure against nucleases

According to Fig. 4, with the neutralization of negative charges of pDNA by the positive charges of the amino groups associated with the chitosan nanocarrier, in both concentrations, the pDNA remained in the well and did not migrate towards the positive electrode. However, naked pDNA and pDNA complexes with the control did not remain in their initial position and migrated throughout the gel due to their non-neutralized charge. The protection of DNA against DNase enzymes, which are present in serum and the extracellular matrix, is a critical parameter in gene transfer¹⁷. The lack of gene detection in agarose gel in samples treated with DNase I demonstrates that the GO-CS@Ca nanocarrier, at both concentrations, has failed to effectively protect pDNA from degradation by serum enzymes.

Cytotoxicity of the GO-CS@Ca nanocarrier

Cationic polymers and lipid-based carriers possess significant advantages and high efficacy, making them attractive alternatives to viral vectors for gene delivery. However, their clinical and in vivo application is often limited due to their cellular toxicity¹⁸. Figure 5 illustrates the cell viability percentage of the MCF-7 cell line after 24 and 48 h of incubation with the GO-CS@Ca nanocarrier and GO-CS@Ca/pDNA nanoplex at various doses. With increasing concentrations of the GO-CS@Ca and GO-CS@Ca/pDNA after transfection, the cell viability percentage decreases. Generally, the range of cell viability percentage after transfection with the GO-CS@Ca is 56.79–87.86%, while with the GO-CS@Ca/pDNA it is 58.88–91.76%.

Apoptosis analysis of the GO-CS@Ca nanocarrier

Apoptosis, also referred to as programmed cell death, is a vital biological process that plays a crucial role in cancer treatment by eliminating cells that have undergone genetic changes within the body¹⁹. Figure 6 illustrates

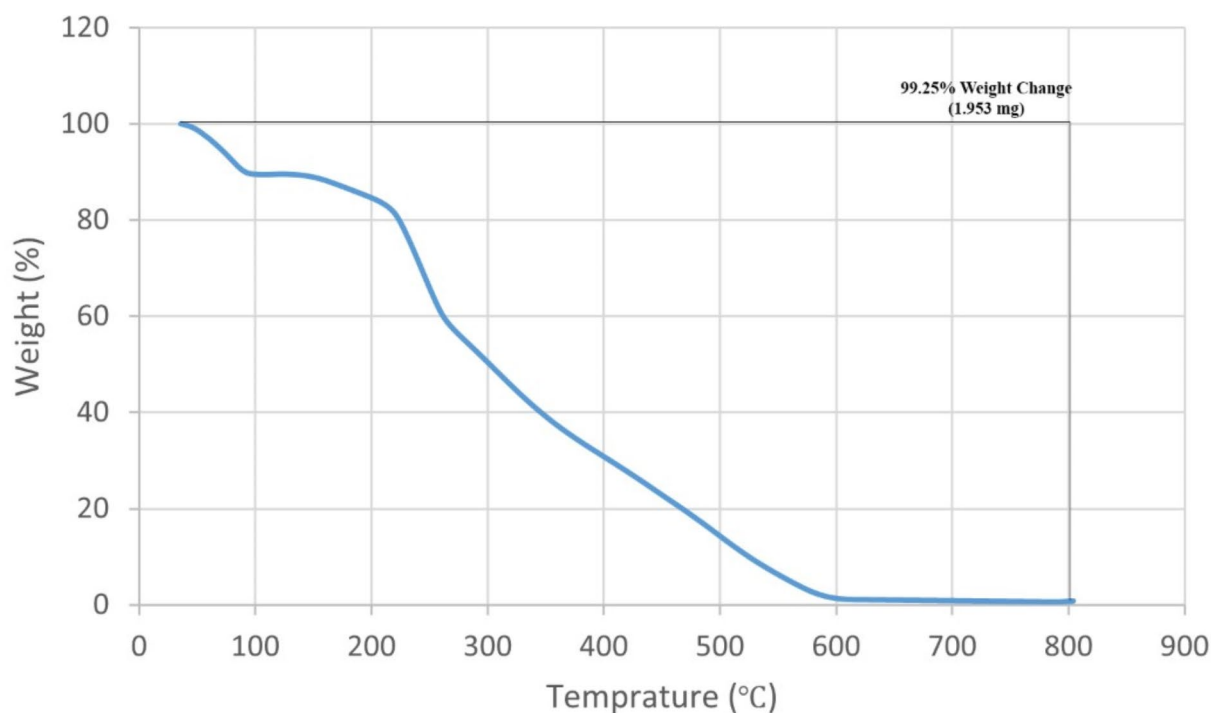


Fig. 3. TGA graph of of GO-CS@Ca.

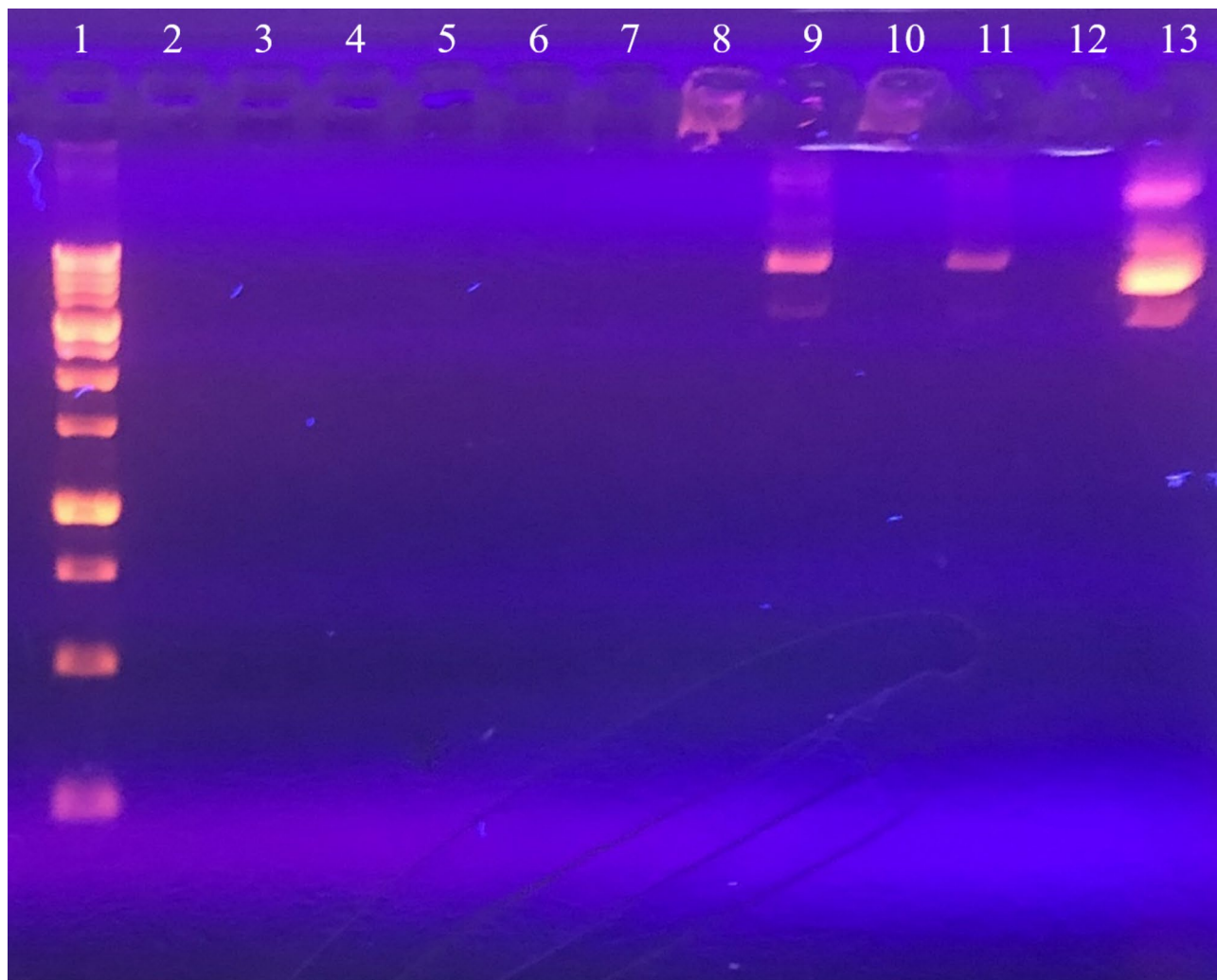


Fig. 4. The ability of the GO-CS@Ca nanocarrier to condense and protect the gene structure against nucleases (1) Ladder, (2) GO-CS@Ca/pDNA treated with DNase, (3) control/pDNA treated with DNase, (4) GO-CS@Ca/pDNA treated with DNase, (5) control/pDNA treated with DNase, (6) GO-CS@Ca treated with DNase, (7) naked pDNA treated with DNase, (8) GO-CS@Ca/pDNA, (9) control/pDNA, (10) GO-CS@Ca/pDNA, (11) control/pDNA, (12) GO-CS@Ca, and (13) naked pDNA.

the distribution of cell populations, including live cells (Q1), cells in late apoptotic stage (Q2), cells in early apoptotic stage (Q3), and necrotic cells (Q4), treated with control (A1), control/pDNA (A2), GO-CS@Ca (A3), and GO-CS@Ca/pDNA (A4). The GO-CS@Ca/pDNA nanoplex demonstrated a higher apoptosis rate (73.3%) compared to the GO-CS@Ca (64.4%), control/pDNA (48.7%), and control (6.82%). This indicates that the BID plasmid DNA, facilitated by the GO-CS@Ca nanocarrier, effectively enters the MCF-7 cancer cell population and induces apoptosis.

Cell cycle analysis of the GO-CS@Ca nanocarrier

During the process of apoptosis, endonucleases cleave the DNA structure of cells, resulting in the generation of fragments approximately 180 to 200 bp in length. Therefore, the sub-G1 peak, observed in the cell cycle analysis graph within the range of 180 to 200 bp, indicates the proportion of cells undergoing apoptosis²⁰. According to Fig. 7, the sub-G1 peak in the GO-CS@Ca/pDNA nanoplex (42.53%) is higher compared to the GO-CS@Ca (13.08%), control/pDNA (11.65%), and control (7.38%). This indicates a greater level of DNA cleavage and a higher incidence of apoptosis induced by the GO-CS@Ca/pDNA.

Transfection analysis of the GO-CS@Ca nanocarrier

Transferring DNA into cells in gene therapy is challenging when using naked DNA, as it faces difficulties in entering the cells. On the other hand, transferring DNA with the help of a positively charged nanocarrier also poses problems, such as protein binding, immune system activation, rapid clearance from the body, and degradation by cellular lysosomes^{21,22}. The fluorescence observed in Fig. 8 indicates the successful cellular

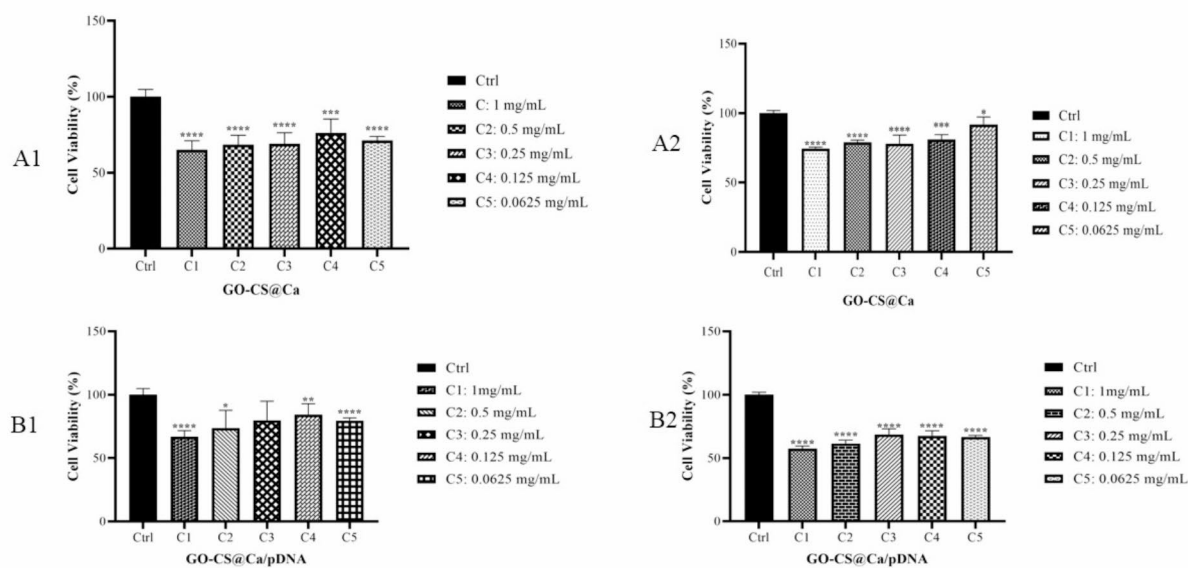


Fig. 5. Cell viability percentage of the MCF-7 cell line in the MTT assay treating with different concentrations of the A) GO-CS@Ca and GO-CS@Ca/pDNA after 24 h (A1 and B1) and 48 h (A2 and B2).

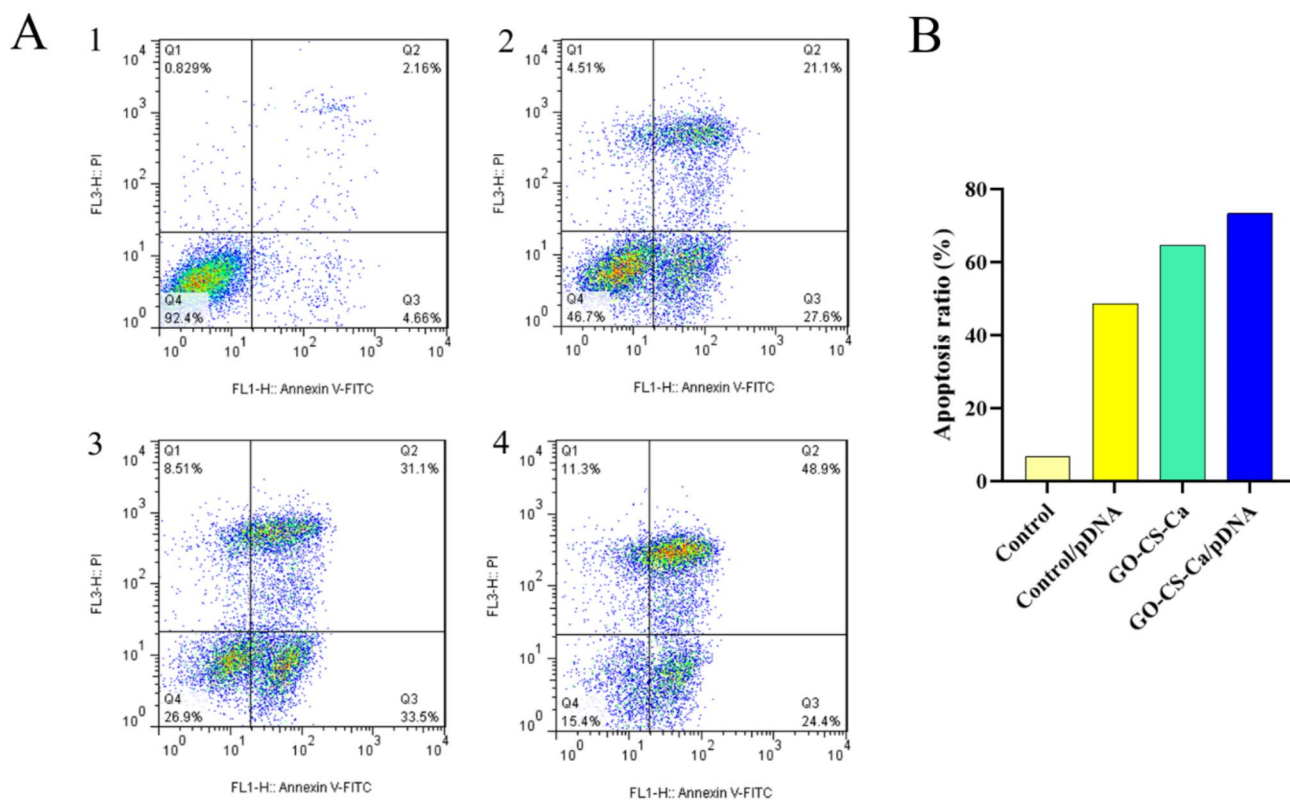


Fig. 6. A) Apoptosis analysis using flow cytometry on MCF-7 cells treated with (1) control, (2) control/pDNA, (3) GO-CS@Ca, (4) GO-CS@Ca/pDNA. B) Apoptosis ratio chart of MCF-7 cells.

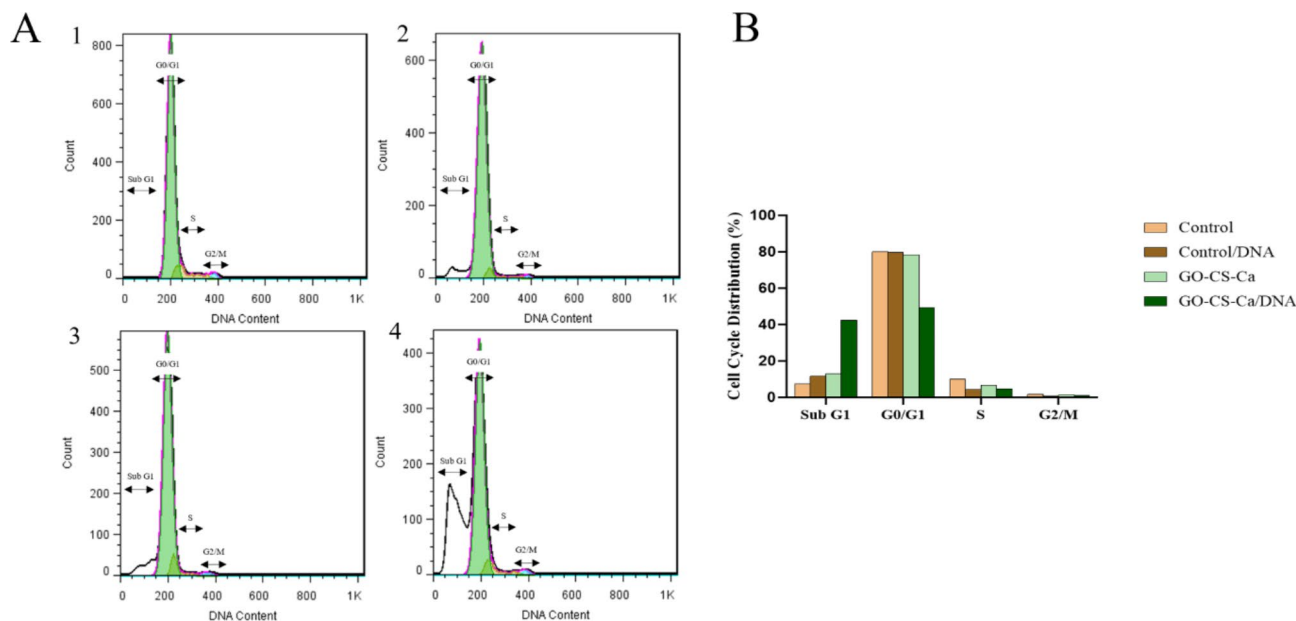


Fig. 7. A) Cell cycle analysis using flow cytometry on MCF-7 cells treated with (1) control, (2) control/pDNA, (3) GO-CS@Ca, (4) GO-CS@Ca/pDNA. B) Cell cycle distribution chart of MCF-7 cells.

transfer of the GO-CS@Ca/pDNA nanoplex and subsequent expression of the GFP plasmid (green fluorescent protein) in the MCF-7 cell line.

Discussion

Developing the drug and gene delivery systems using nanotechnology is essential for reducing side effects in normal cells and enhancing specific targeting of tumor cells in cancer treatment²³.

In gene delivery, two categories of vectors, viral and non-viral vectors, can be utilized to transfer the desired gene into cancer cells²⁴. Non-viral vectors, such as lipids and cationic polymers, offer advantages such as reduced immunogenicity, cost-effectiveness, ease of production, and high gene transfer capacity compared to viral vectors²⁵. However, one of the significant drawbacks of cationic polymer-based carriers used in gene delivery systems is their high toxicity for clinical applications¹⁸.

Chitosan is a natural amino polysaccharide that is used due to its high efficiency, low cost, biodegradability, and water solubility in gene delivery systems. It has been observed that chitosan is biocompatible and has very low toxicity. For example, in a study conducted by Mao and colleagues in 2004, it was found that chitosan is non-toxic up to a concentration of 1 mg/ml^{26,27}. Similarly, in a study by Rejirold and colleagues in 2010, it was observed that chitosan nanoparticles at concentrations ranging from 0.1 to 1 mg/ml have no cellular toxicity on cell lines such as L929, NIH-3T3, PC3, and KB²⁸.

Despite the unique and diverse properties of graphene oxide, its use in cancer treatment through drug delivery and gene delivery raises concerns due to potential toxicity^{29,30}. In a study conducted by Saravanabhavan and colleagues in 2019, which focused on the graphene oxide-chitosan complex, it was found that this carrier has low toxicity (cell viability above 55%). However, it has been noted that carbon-based materials like graphene oxide can create false results by interfering with the marker of the MTT test (formazan). Therefore, to evaluate the cellular toxicity of this carrier, the researchers measured ROS activity in addition to the MTT test in this study. It was observed that the ROS activity in cells exposed to the GO-CS carrier was at a moderate level, indicating consistency with the results of the MTT test. On the other hand, the researchers in this study claimed that using equal concentrations of chitosan graphene oxide conjugate prevents interference with a marker of the MTT test by graphene oxide³¹. In this study, the MTT test was employed to investigate the biocompatibility of the synthesized nanocarrier, GO-CS@Ca. It was determined that both GO-CS@Ca and GO-CS@Ca/pDNA complexes are biocompatible and exhibit low cytotoxicity. However, the GO-CS@Ca/pDNA complex showed lower toxicity compared to the GO-CS@Ca nanocomposite itself. In this study, the amounts of chitosan used to prepare the GO-CS@Ca nanocarrier were five times greater than the amounts of graphene oxide, suggesting that graphene oxide did not interfere with the marker of the MTT test, according to the study conducted by Saravanabhavan³¹ and colleagues.

Chitosan is considered a cationic polymer that can effectively interact with anionic plasmid DNA due to its positive charge, compacting the DNA. The compacted plasmid DNA can be protected against serum nucleases and easily transfected into cells through endocytosis^{27,32}. It has also been observed that metal ions, particularly calcium, can enhance gene delivery systems due to their positive charge³³. In the case of the investigated nanocarrier, GO-CS@Ca, the presence of cationic factors such as chitosan and Ca²⁺ renders it positively charged, which is confirmed by the zeta potential analysis (+92.8 mV). According to the gel retardation analysis, the nanocarrier under study can effectively neutralize and condense the negative charges of plasmid DNA.

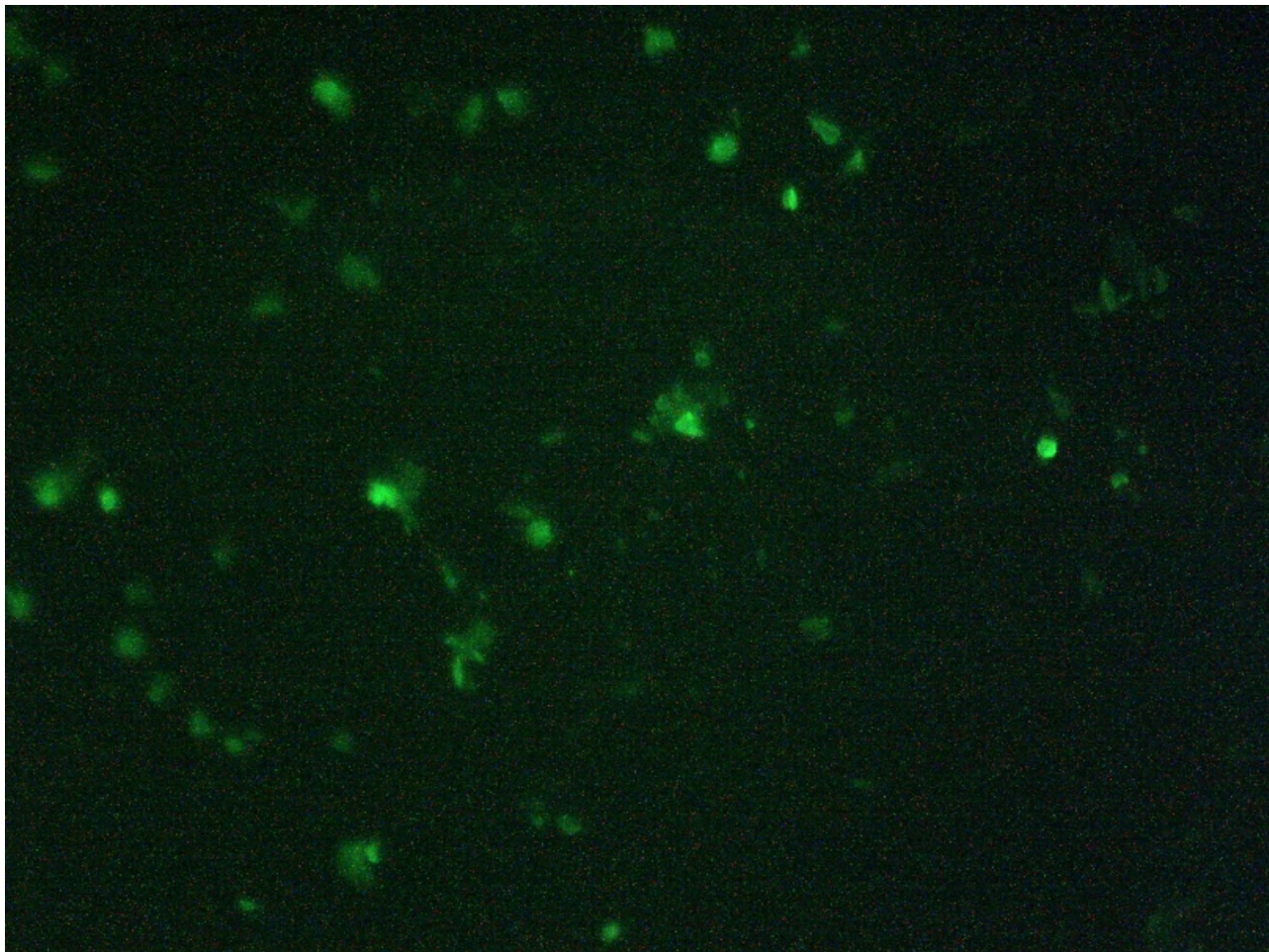


Fig. 8. Fluorescence image of MCF-7 cells transfected with GO-CS@Ca/GFP plasmid.

DNase enzymes present in blood and body fluids are responsible for hydrolyzing the phosphodiester bonds of DNA molecules, preventing immune reactions in the body. Therefore, using naked pDNA for cancer treatment is not suitable due to their degradation by nucleases. As a result, the desired DNA needs to be encapsulated by a nanocarrier. In the study conducted by Mao and colleagues in 2000 on chitosan-DNA nanoparticles, it was observed that the encapsulation of DNA with chitosan protected against degradation by serum nucleases³⁴. According to the findings of Huo and colleagues in 2018 on graphene oxide, it was observed that graphene oxide can interact with the active site of the deoxyribonuclease (DNase) and inhibit its activity, thus protecting DNA from degradation. Therefore, based on these studies, it was expected that the GO-CS@Ca nanocarrier could also protect pDNA from serum nucleases.

Cancer cells, due to their ability to evade the process of cellular apoptosis, can persist and grow uncontrollably. Therefore, targeting apoptosis has become one of the principal methods for treating various types of cancer. According to the results of apoptosis by flow cytometry analysis in this study, the GO-CS@Ca nanocarrier was able to effectively deliver the pro-apoptotic gene BID into the MCF-7 cell line and induce significant apoptosis in these cells. Furthermore, it has been observed that during the process of apoptosis, the enzyme CAD (Caspase Activated DNase) is activated by caspase 3 and rapidly cleaves DNA into fragments of 180 to 200 base pairs. The results of the cell cycle by flow cytometry analysis in this study also confirmed that the GO-CS@Ca nanocarrier was able to effectively deliver the plasmid DNA encoding BID into the MCF-7 cell line, increasing to the Sub G1 peak, which corresponds to the fragments of 180 to 200 base pairs in the cell cycle profile.

Finally, a transfection assay was performed to confirm the successful delivery of the synthesized nanocarrier to the cell nucleus. It was determined that the GFP gene was successfully delivered into the MCF-7 cell line using the GO-CS@Ca nanocarrier, and upon expression, it emitted fluorescence under a microscope, indicating successful transfection.

Conclusion

This study aimed to synthesize, characterize, and investigate a novel nanocarrier, GO-CS@Ca, for gene delivery to the MCF-7 cell line for breast cancer treatment. The results of this study demonstrated that GO-CS@Ca is a biocompatible nanocarrier with low toxicity that effectively neutralizes and condenses the target gene.

Additionally, this nanocarrier successfully delivered the pro-apoptotic gene to cancer cells and induced apoptosis. Lastly, it was observed that the GO-CS@Ca nanocarrier can successfully transfect genes into the cell nucleus.

Data availability

All data are available via the corresponding author.

Received: 4 March 2024; Accepted: 5 November 2024

Published online: 10 November 2024

References

- Giaquinto, A. N. et al. Breast cancer statistics, 2022. *Cancer J. Clin.* **72**(6), 524–541 (2022).
- Casais-Molina, M., Cab, C., Canto, G., Medina, J. & Tapia, A. Carbon nanomaterials for breast cancer treatment. *J. Nanomaterials*. **2018**, 1–9 (2018).
- Tilsed, C. M., Fisher, S. A., Nowak, A. K., Lake, R. A. & Lesterhuis, W. J. Cancer chemotherapy: insights into cellular and tumor microenvironmental mechanisms of action. *Front. Oncol.* **12**, 960317 (2022).
- Liu, Y. P. et al. Molecular mechanisms of chemo- and radiotherapy resistance and the potential implications for cancer treatment. *MedComm.* **2**(3), 315–340 (2021).
- Redmond, K. M., Wilson, T. R., Johnston, P. G. & Longley, D. B. Resistance mechanisms to cancer chemotherapy. *Front. Biosci.* **13**, 5138–5154 (2008).
- Rajaei, M. et al. Chitosan/agarose/graphene oxide nanohydrogel as drug delivery system of 5-fluorouracil in breast cancer therapy. *J. Drug Deliv. Sci. Technol.* **82**, 104307 (2023).
- Alshareeda, A. T., Khatijah, M. N., Al-Sowayan, B. S. & Nanotechnology A revolutionary approach to prevent breast cancer recurrence. *Asian J. Surg.* **46**(1), 13–17 (2023).
- Gómez-Navarro, J., Arafat, W. & Xiang, J. Gene therapy for carcinoma of the breast: pro-apoptotic gene therapy. *Breast Cancer Res.* **2**(1), 1–13 (1999).
- Nayerossadat, N., Maedeh, T. & Ali, P. A. Viral and nonviral delivery systems for gene delivery. *Adv. Biomedical Res.* **1**. (2012).
- Qian, S. et al. The role of BCL-2 family proteins in regulating apoptosis and cancer therapy. *Front. Oncol.* **12**, 985363 (2022).
- Chen, B. et al. Polyethylenimine-functionalized graphene oxide as an efficient gene delivery vector. *J. Mater. Chem.* **21**(21), 7736–7741 (2011).
- Priyadarsini, S., Mohanty, S., Mukherjee, S., Basu, S. & Mishra, M. Graphene and graphene oxide as nanomaterials for medicine and biology application. *J. Nanostructure Chem.* **8**, 123–137 (2018).
- Orecchioni, M., Cabizza, R., Bianco, A. & Delogu, L. G. Graphene as cancer theranostic tool: progress and future challenges. *Theranostics.* **5**(7), 710 (2015).
- Wang, C., Chen, B., Zou, M. & Cheng, G. Cyclic RGD-modified chitosan/graphene oxide polymers for drug delivery and cellular imaging. *Colloids Surf., B* **122**, 332–340 (2014).
- Hashemi, E. et al. Graphene oxide negatively regulates cell cycle in embryonic fibroblast cells. *Int. J. Nanomed.* :6201–6209. (2020).
- Danaei, M. et al. Impact of particle size and polydispersity index on the clinical applications of lipidic nanocarrier systems. *Pharmaceutics.* **10**(2), 57 (2018).
- Duan, X. et al. Amphiphilic graft copolymer based on poly (styrene-co-maleic anhydride) with low molecular weight polyethylenimine for efficient gene delivery. *Int. J. Nanomed.*, 4961–4972. (2012).
- Lv, H., Zhang, S., Wang, B., Cui, S. & Yan, J. Toxicity of cationic lipids and cationic polymers in gene delivery. *J. Controlled Release* **114**(1), 100–109 (2006).
- Sankari, S. L., Masthan, K., Babu, N. A., Bhattacharjee, T. & Elumalai, M. Apoptosis in cancer—an update. *Asian Pac. J. Cancer Prev.* **13**(10), 4873–4878 (2012).
- Rashidi, M. et al. Selective cytotoxicity and apoptosis-induction of *Cyrtopodium scabrum* extract against digestive cancer cell lines. *Int. J. Cancer Manage.* **10**(5). (2017).
- Ogris, M. & Wagner, E. Targeting tumors with non-viral gene delivery systems. *Drug Discovery Today* **7** (8), 479–485 (2002).
- Afrouz, M. et al. Preparation and characterization of magnetic PEG-PEI-PLA-PEI-PEG/Fe₃O₄-PCL/DNA micelles for gene delivery into MCF-7 cells. *J. Drug Deliv. Sci. Technol.* **79**, 104016 (2023).
- Mokhtarzadeh, A. et al. Targeted gene delivery to MCF-7 cells using peptide-conjugated polyethylenimine. *AAPS PharmSciTech.* **16**, 1025–1032 (2015).
- Mali, S. Delivery systems for gene therapy. *Indian J. Hum. Genet.* **19**(1), 3 (2013).
- Ramamoorthi, M. & Narvekar, A. Non viral vectors in gene therapy—an overview. *J. Clin. Diagn. Research: JCDR* **9**(1), GE01 (2015).
- Mao, S. et al. The depolymerization of chitosan: effects on physicochemical and biological properties. *Int. J. Pharm.* **281**(1–2), 45–54 (2004).
- Lee, M.-K. et al. The use of Chitosan as a condensing agent to enhance emulsion-mediated gene transfer. *Biomaterials* **26**(14), 2147–2156 (2005).
- Rejinold, N. S. et al. Saponin-loaded chitosan nanoparticles and their cytotoxicity to cancer cell lines in vitro. *Carbohydr. Polym.* **84**(1), 407–416 (2011).
- Chung, C. et al. Biomedical applications of graphene and graphene oxide. *Acc. Chem. Res.* **46**(10), 2211–2224 (2013).
- Rhazouani, A. et al. Synthesis and toxicity of graphene oxide nanoparticles: A literature review of in vitro and in vivo studies. *BioMed Research International.* 2021 (2021).
- Saravanabhavan, S. S. et al. Graphene oxide functionalized with chitosan based nanoparticles as a carrier of siRNA in regulating Bcl-2 expression on Saos-2 & MG-63 cancer cells and its inflammatory response on bone marrow derived cells from mice. *Mater. Sci. Engineering: C* **99**, 1459–1468 (2019).
- Dunlap, D. D., Maggi, A., Soria, M. R. & Monaco, L. Nanoscopic structure of DNA condensed for gene delivery. *Nucleic Acids Res.* **25**(15), 3095–3101 (1997).
- Kulkarni, V. I., Shenoy, V. S., Dodiya, S. S., Rajyaguru, T. H. & Murthy, R. R. Role of calcium in gene delivery. *Expert Opin. Drug Deliv.* **3**(2), 235–245 (2006).
- Mao, H.-Q. et al. Chitosan-DNA nanoparticles as gene carriers: synthesis, characterization and transfection efficiency. *J. Controlled Release* **70**(3), 399–421 (2001).

Author contributions

—The conception and design of the study: F.N and A.F; acquisition of data, analysis, and interpretation of data: F.N, A.D, A.F, and M.T; drafting of the article: A.D and F.N; revising the article critically for important intellectual content, final approval of the version to be submitted: F.N, A.F. All authors read and approved the final version of the manuscript.

Funding

This work was supported financially by Hamadan University of Medical Sciences, Hamadan, Iran (Grant Numbers: 140008186870).

Declarations

Competing interests

The authors declare no competing interests.

Ethical approval and consent to participate

This study has been approved by the Ethics Committee of Hamadan University of Medical Sciences, Hamadan, Iran (IR.UMSHA.REC.1400.545).

Additional information

Correspondence and requests for materials should be addressed to F.N.

Reprints and permissions information is available at www.nature.com/reprints.

Publisher's note Springer Nature remains neutral with regard to jurisdictional claims in published maps and institutional affiliations.

Open Access This article is licensed under a Creative Commons Attribution-NonCommercial-NoDerivatives 4.0 International License, which permits any non-commercial use, sharing, distribution and reproduction in any medium or format, as long as you give appropriate credit to the original author(s) and the source, provide a link to the Creative Commons licence, and indicate if you modified the licensed material. You do not have permission under this licence to share adapted material derived from this article or parts of it. The images or other third party material in this article are included in the article's Creative Commons licence, unless indicated otherwise in a credit line to the material. If material is not included in the article's Creative Commons licence and your intended use is not permitted by statutory regulation or exceeds the permitted use, you will need to obtain permission directly from the copyright holder. To view a copy of this licence, visit <http://creativecommons.org/licenses/by-nc-nd/4.0/>.

© The Author(s) 2024